Proceedings of 10th Annual Workshop on CFD Application in Propulsion,
NASA Marshall Space Flight Center, Huntsville, AL, April 28-30, 1992.

Inverse Design of a Proper Number, Shapes, Sizes, and Locations of Coolant Flow Passages

George S. Dulikravich
Department of Aerospace Engineering, 233 Hammond Building
The Pennsylvania State University, University Park, PA 16802, USA

During the past several years we have developed an inverse method that allows a thermal cooling system designer to determine proper sizes, shapes, and locations of coolant passages (holes) in, say, an internally cooled turbine blade, a scram jet strut, a rocket chamber wall, etc. Using this method the designer can enforce a desired heat flux distribution on the hot outer surface of the object, while simultaneously enforcing desired temperature distributions on the same hot outer surface as well as on the cooled interior surfaces of each of the coolant passages. This constitutes an over-specified problem which is solved by allowing the number, sizes, locations and shapes of the holes to adjust iteratively until the final internally cooled configuration satisfies the over-specified surface thermal conditions and the governing equation for the steady temperature field.

The problem is solved by minimizing an error function expressing the difference between the specified and the computed hot surface heat fluxes. The computed outer surface heat flux q_{out}^{comp} will not be the same as the specified outer surface heat flux, q_{out}^{spec}. A properly scaled L-2 norm of the difference between the specified outer surface heat flux, q_{out}^{spec}, and the computed outer surface heat flux, q_{out}^{comp}, is then minimized by iteratively changing the sizes, shapes, and locations of coolant passages. Starting with a large number of guessed holes, all unnecessary coolant passages are efficiently eliminated when their sizes reduce below a prespecified minimal allowable value. The minimization has been performed automatically using a standard optimization algorithm of Davidon-Fletcher-Powell. Local minimas in the optimization process were successfully avoided by changing the formulation for the objective function whenever the local minimas were detected. The temperature field analysis was performed using our highly accurate boundary integral element code with linearly varying temperature along straight surface panels. Examples of the inverse design applied to internally cooled turbine blades and scram jet struts (coated and non-coated) having circular and non-circular coolant flow passages will be shown.

1. Mathematical model

Steady heat conduction in internally cooled objects is modeled as a boundary value problem for Laplace's equation over a multiply-connected domain.

Assumptions are:
- temperature field is steady
- solid material of the blade is thermally isotropic.
- thermal expansion is neglected

Governing equation is Laplace's equation:

$$\boxed{\nabla^2 T = 0} \qquad (1)$$

2. Objectives

Determine:
- the exact number of the holes,
- radii of the holes,
- locations of the holes,

such that relative error between specified and computed heat fluxes at the outer boundary is minimized.

3. Boundary Conditions - Ill Posed Boundary Value Problem

Both, Dirichlet and Neumann boundary conditions are specified on the outer boundary. Such an overspecified problem can be solved by inverse (design) approach. The problem is solvable since the domain is multi-connected: positions, shapes and dimensions of the holes will provide additional degrees of freedom.

4. Constraints

Besides minimizing the heat flux error, optimized shape has to satisfy these constraints:
- minimum distance between holes,
- minimum distance between holes and the outer boundary

5. Objective Functions

Two different definitions of objective function were used. The difference between the specified and the heat flux and heat flux obtained by the current design can be computed as a global error:

$$F_1(\mathbf{x}) = \frac{\sum_{j=1}^{N}(q_j^c - q_j^r)^2}{\sum_{j=1}^{N}(q_j^r)^2} \tag{2}$$

or as a local error in heat flux at each node:

$$F_2(\mathbf{x}) = \sum_{j=1}^{N} \frac{(q_j^c - q_j^r)^2}{(q_j^r)^2} \tag{3}$$

Two constraints were incorporated into the objective function using a barrier function

$$B(\mathbf{g}(\mathbf{x}), w_b) = \frac{1}{w_b} \sum_{i=1}^{M} \left[\sum_{j=1}^{N_2} \frac{d^s}{\left(D_j^s - d^s - r_i\right)} + \sum_{k=1}^{M} \frac{d^h}{\left(D_k^h - d^h - r_i - r_k\right)} \right] \tag{4}$$

The composite objective function can have two forms:

$$F_i(\mathbf{g}(\mathbf{x}), w_b) = F_i(\mathbf{x}) + B(\mathbf{g}(\mathbf{x}), w_b), \quad i = 1, 2 \tag{5}$$

depending whether global or local objective function is used for its evaluation.

2. The Optimization Procedure

The optimization procedure consists of the following steps:

(1) Specify shape of the outer surface and coating of the turbine blade.

(2) Specify desired temperature T_j^r values on the outer and inner surfaces.

(3) Specify desired heat flux q_j^r values on the outer surface.

(4) Specify manufacturing constraints:
(i) minimum distance d^s between holes and the outer surface,
(ii) minimum distance d^h between any two neighboring holes.

(5) Specify initial guess for the number of holes, M, their dimensions, r_i, and locations of the centers of the holes, x_i and y_i. Thus, there will be 3×M design variables if we limit ourselves to circular holes only.

(6) Using the Boundary Element Method, the Laplace's equation for a given domain and temperature boundary conditions is solved and heat fluxes at the outer boundary are computed. The Laplace's equation is solved 3×M times, ones for each perturbed design variable to compute the gradient.

(7) Determine relative error between specified and computed heat fluxes and evaluate the objective function. At the same time the barierr function has to be evaluated to determine the composite objective function F_i.

(8) Davidon-Powel-Fletcher technique is used to find the new values of design variables repeating the optimization procedure from the step (6) until the corresponding composite objective function F is less than a prespecified value If the dimension of a hole becomes less than a prespecified value, the hole is eliminated from further optimization. If the optimization procedure stalls in a local minimum the objective function formulation is changed from Eq. 2 to Eq. 3 while continuing with optimization from the step (6).

References

Kennon, S.R. and Dulikravich, G.S., (1985), "The Inverse Design of Internally Cooled Turbine Blades," *ASME Journal of Eng. Gas Turbines and Power*, January 1985, pp. 123-126.

Kennon, S.R. and Dulikravich, G.S., (1986a), "Inverse Design of Multiholed Internally Cooled Cooled Turbine Blades," *Int. Jour. of Num. Meth. in Eng.*, Vol. 22, pp. 363-375.

Kennon, S. R. and Dulikravich, G. S. (1986b), "Inverse Design of Coolant Flow Passages Shapes With Partially Fixed Internal Geometries," *International Journal ofTurbo & Jet Eng.*, Vol. 3, (1), pp. 13-20.

Chiang, T.L. and Dulikravich, G.S., (1986), "Inverse Design of Composite Turbine Blade Circular Coolant Flow Passages," *ASME Journal of Turbomachinery*, Vol. 108, pp. 275-282.

Dulikravich, G.S., (1988), "Inverse Design and Active Control Concepts in Strong Unsteady Heat Conduction," *Applied Mechanics Reviews,* Vol. 41, No. 6, June 1988, pp. 270-277.

Dulikravich, G.S. and Kosovic, B., (1991), "Minimization of the Number of Cooling Holes in Internally Cooled Turbine Blades", ASME paper 91-GT-103, ASME Gas Turbine Conference, Orlando, FL, June 2-6, 1991; also to appear in *Internat. Jour. of Turbo & Jet Engines*, 1992.

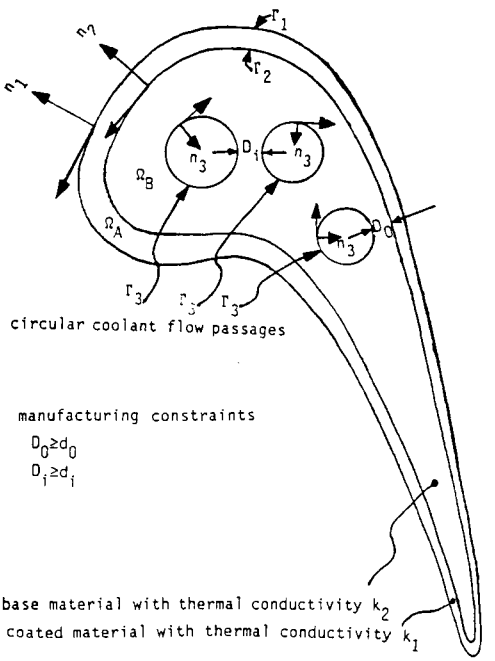

Fig. 1 Geometry and manufacturing constraints

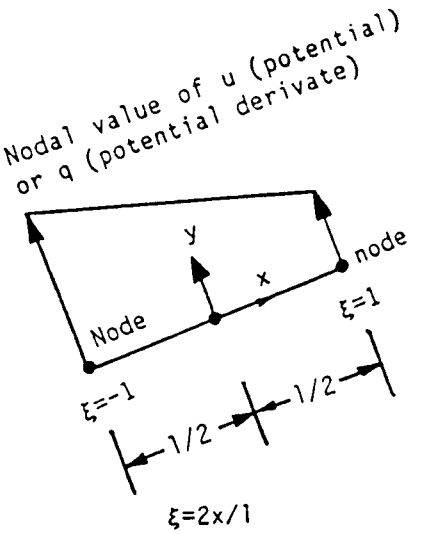

Fig. 2b Linear element

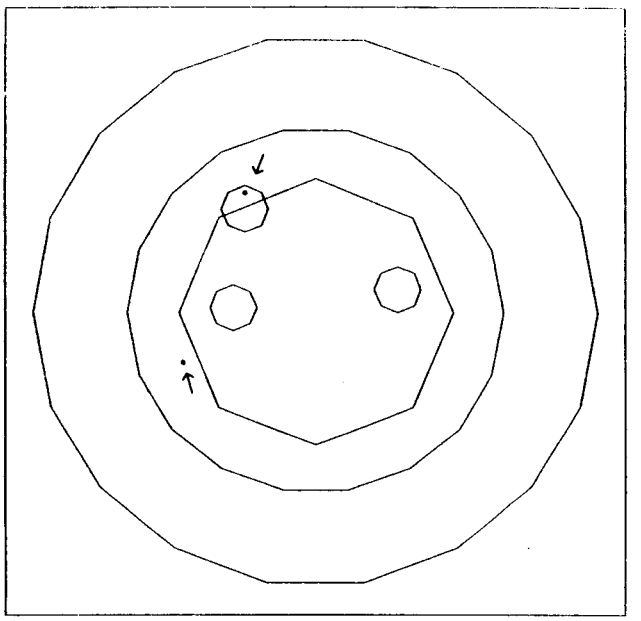

Fig. 1.1 Initial configuration (three holes) and final configuration (one large centrally located hole and two dots marked with arrows) corresponding to a solution with 0.1% integrated flux error.

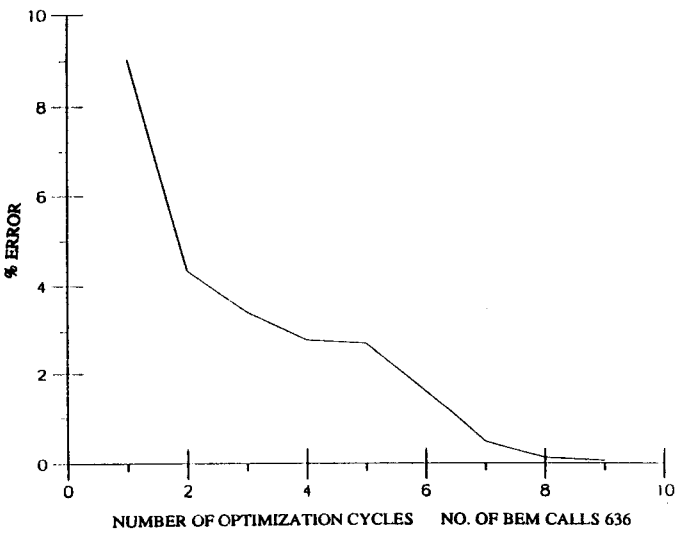

Fig. 1.2 Integrated heat flux error (L_2 norm) convergence history during the optimization.

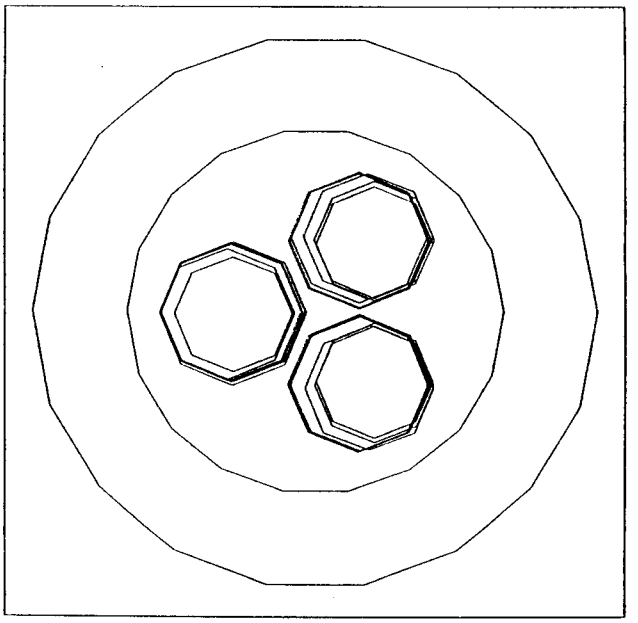

Fig. 1.3 Initially symmetrically located holes of identical size maintain a symmetric configuration throughout the iterative process.

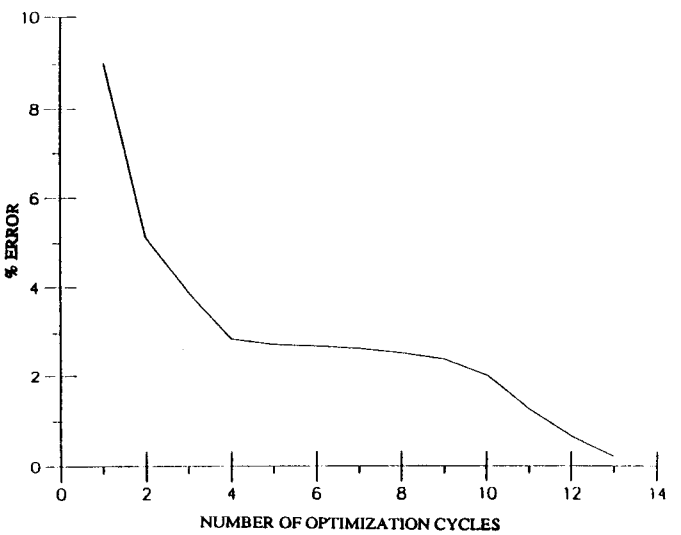

Fig. 1.4 Convergence history of the three-hole symmetrical configuration.

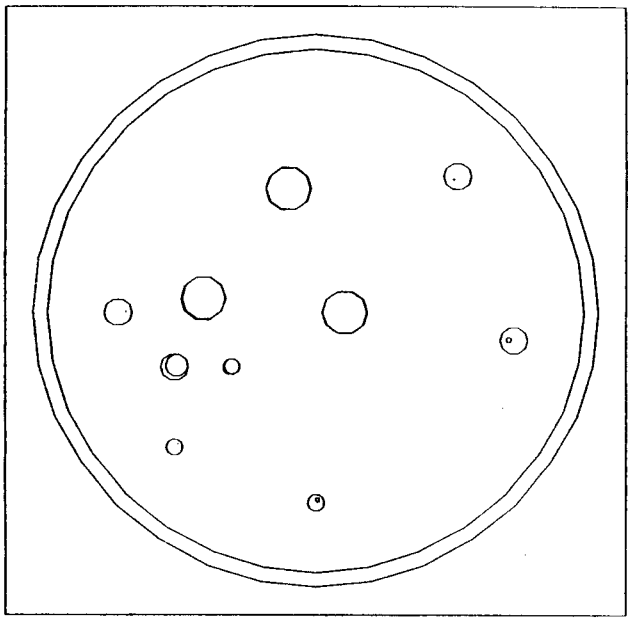

Fig. 1.5 Coated disk problem with initially ten holes. Convergence history shows five holes are reduced to zero. Hole elimination method was not used.

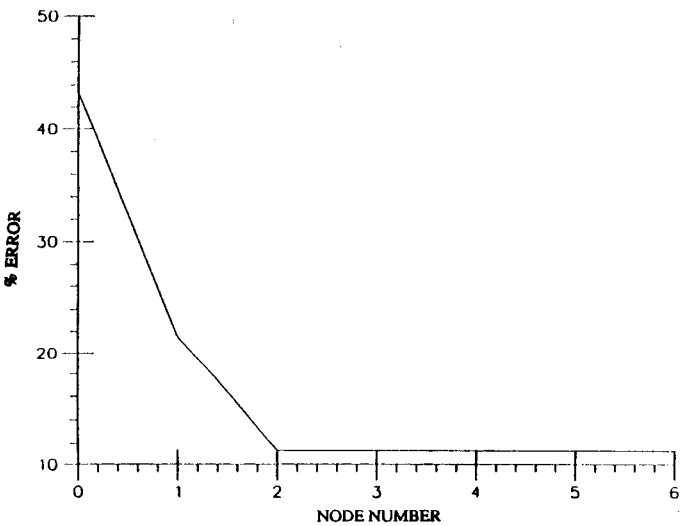

Fig. 1.6 Convergence history for a circular domain with initially ten holes. Hole elimination method was not used. Minimization process terminates in a local minimum.

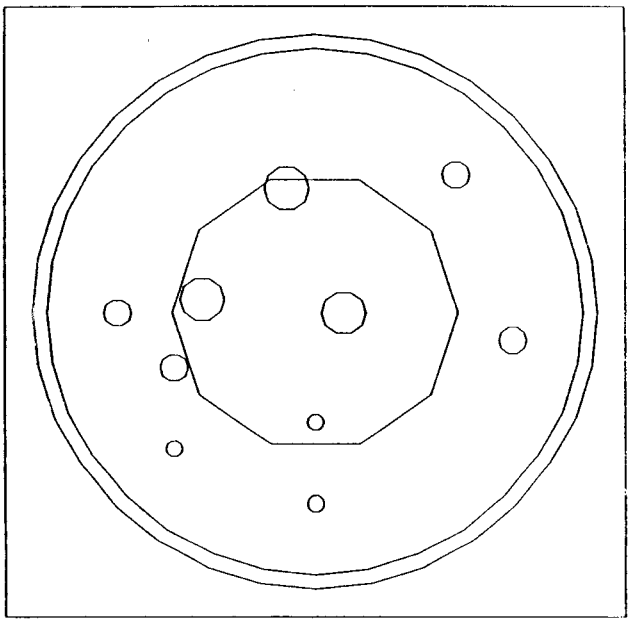

Fig. 1.7 Coated disk problem with initially ten holes. Hole elimination method was used together with objective function switching.

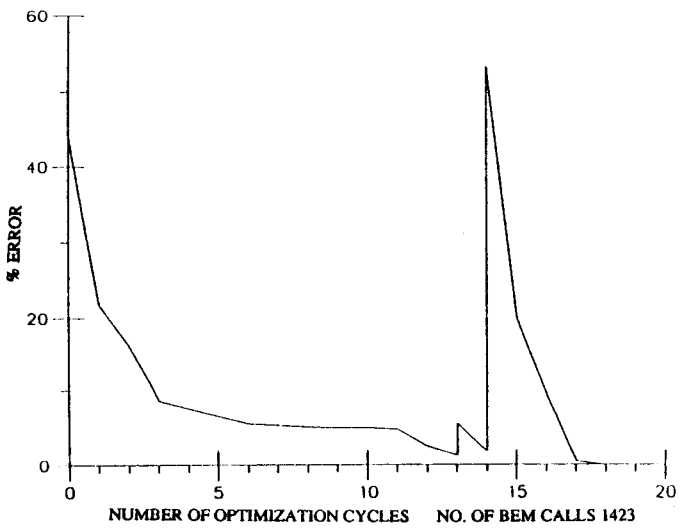

Fig. 1.8 Convergence history for a circular domain with initially ten holes when hole elimination method is applied together with objective function switching. Discontinuities represent changing of the objective function.

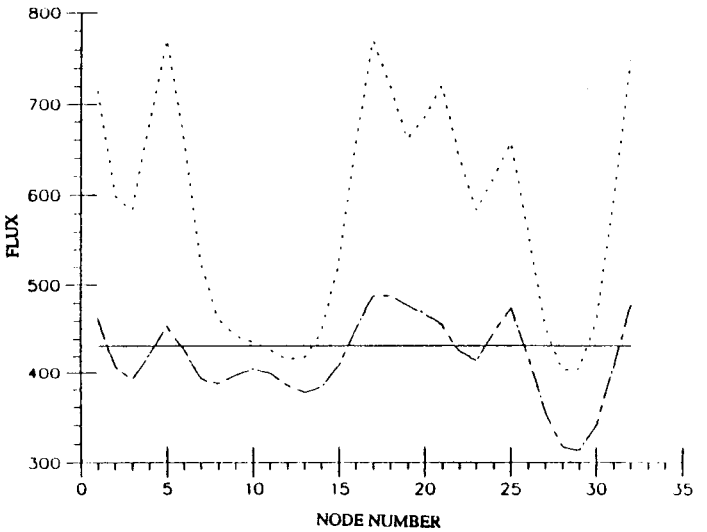

Fig. 1.9 Initial (·····), intermediate (– · – · –) and final (––––––) heat flux distribution through the outer boundary for a cylinder with ten holes initially. Hole elimination method was not used.

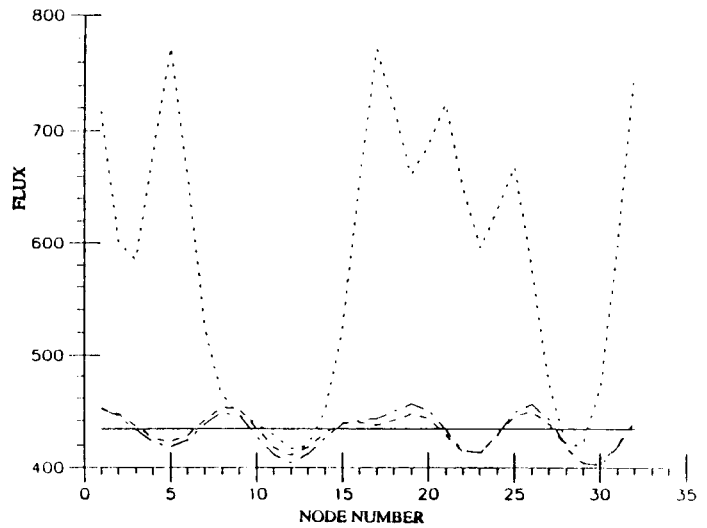

Fig. 1.10 Initial (·····), after 5 cycles (– · – · –) , after 10 cycles (– – – –) and final (———) heat flux distribution through the outer boundary for a cylinder with ten holes initially. Hole elimination method and objective function switching was used.

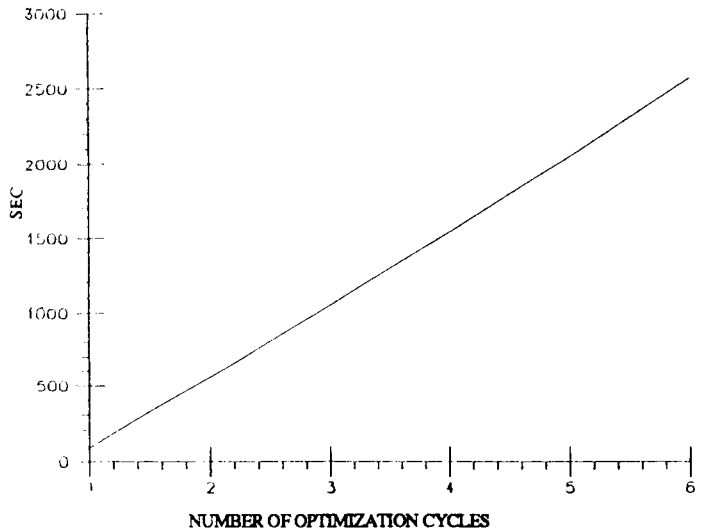

Fig. 1.11 Total CPU time (IBM 3090) vs. number of iterations for a circular cylinder with ten holes initially. Hole elimination method was not applied. Total number of analysis code calls (BEM code) was 1428.

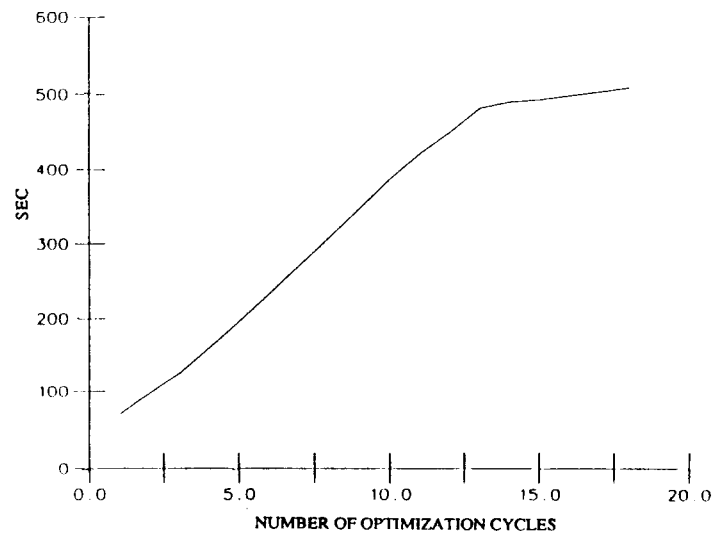

Fig. 1.12 Total CPU time (IBM 3090) vs. number of iterations for a circular cylinder with ten holes initially when hole elimination method was applied together with objective function switching.

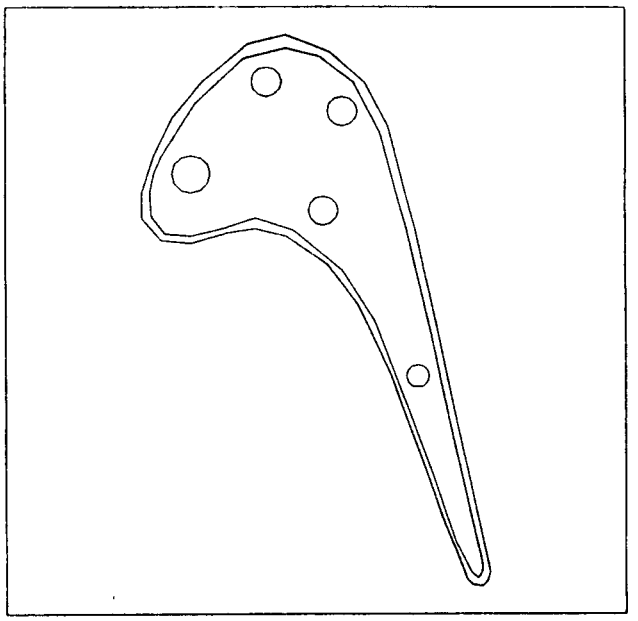

Fig. 1.13 A five-hole coated turbine blade from which thermal boundary conditions were used represents an actual solution for the case of the turbine blade with ten holes initially

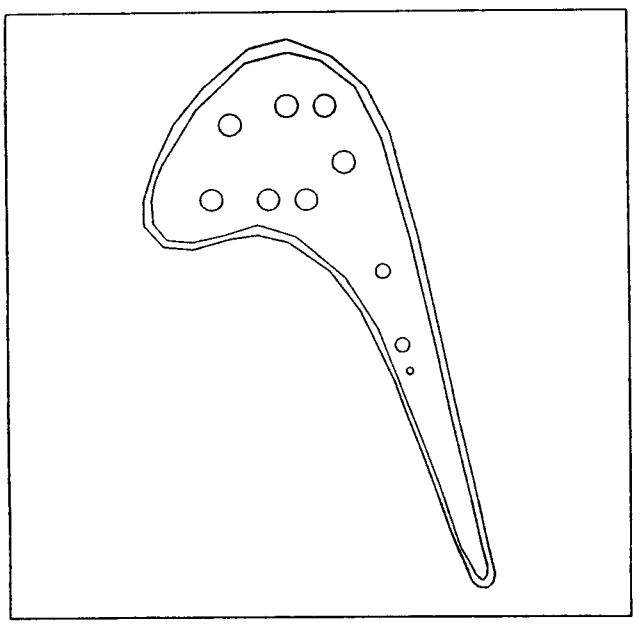

Fig. 1.14 Initial guess for a coated turbine blade configuration with ten holes using thermal boundary conditions from the five-hole configuration

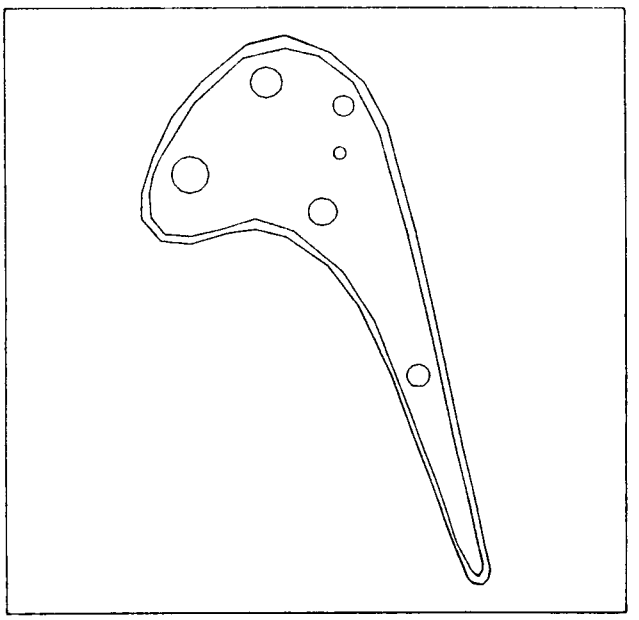

Fig. 1.15 Optimized solution for initial configuration with ten holes. Number of holes is minimized to six, where the sixth hole continues to shrink. Hole elimination method was used together with objective function switching.

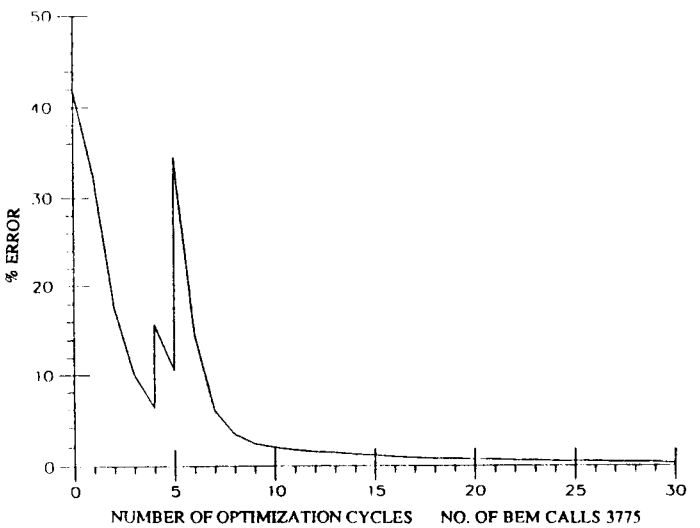

Fig. 1.16 Convergence history for a coated turbine blade with ten holes initially when hole elimination method was applied together with objective function switching. Discontinuities represent changing of the objective function.

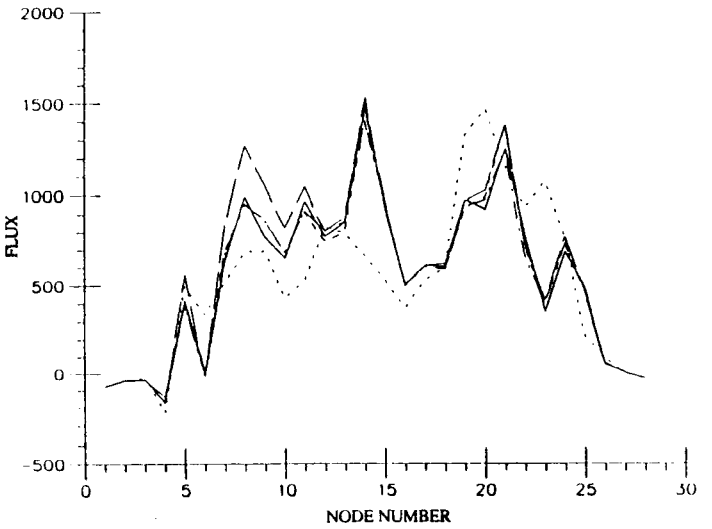

Fig. 1.17 Initial (·····), after 5 cycles (– – – –) , after 10 cycles (– · – · –) and final (————) heat flux distribution through the outer boundary for a turbine blade with initially ten holes. Hole elimination method was used together with objective function switching.

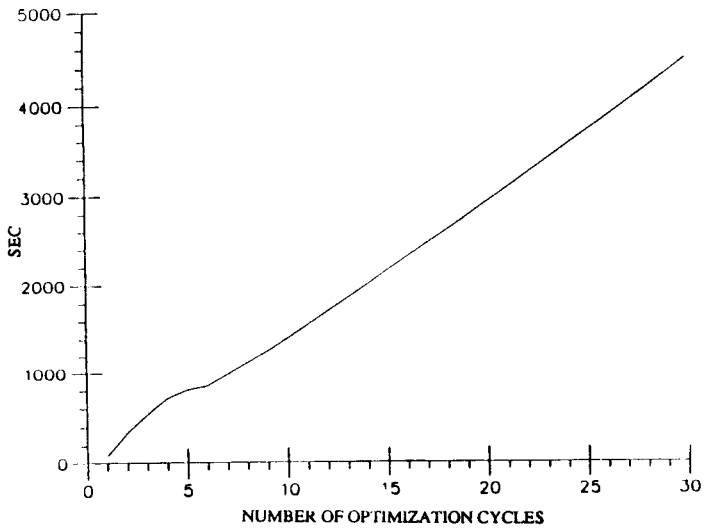

Fig. 1.18 Total CPU time (IBM 3090) vs. number of iterations for a turbine blade with ten holes initially. Hole elimination method was applied together with objective function switching.

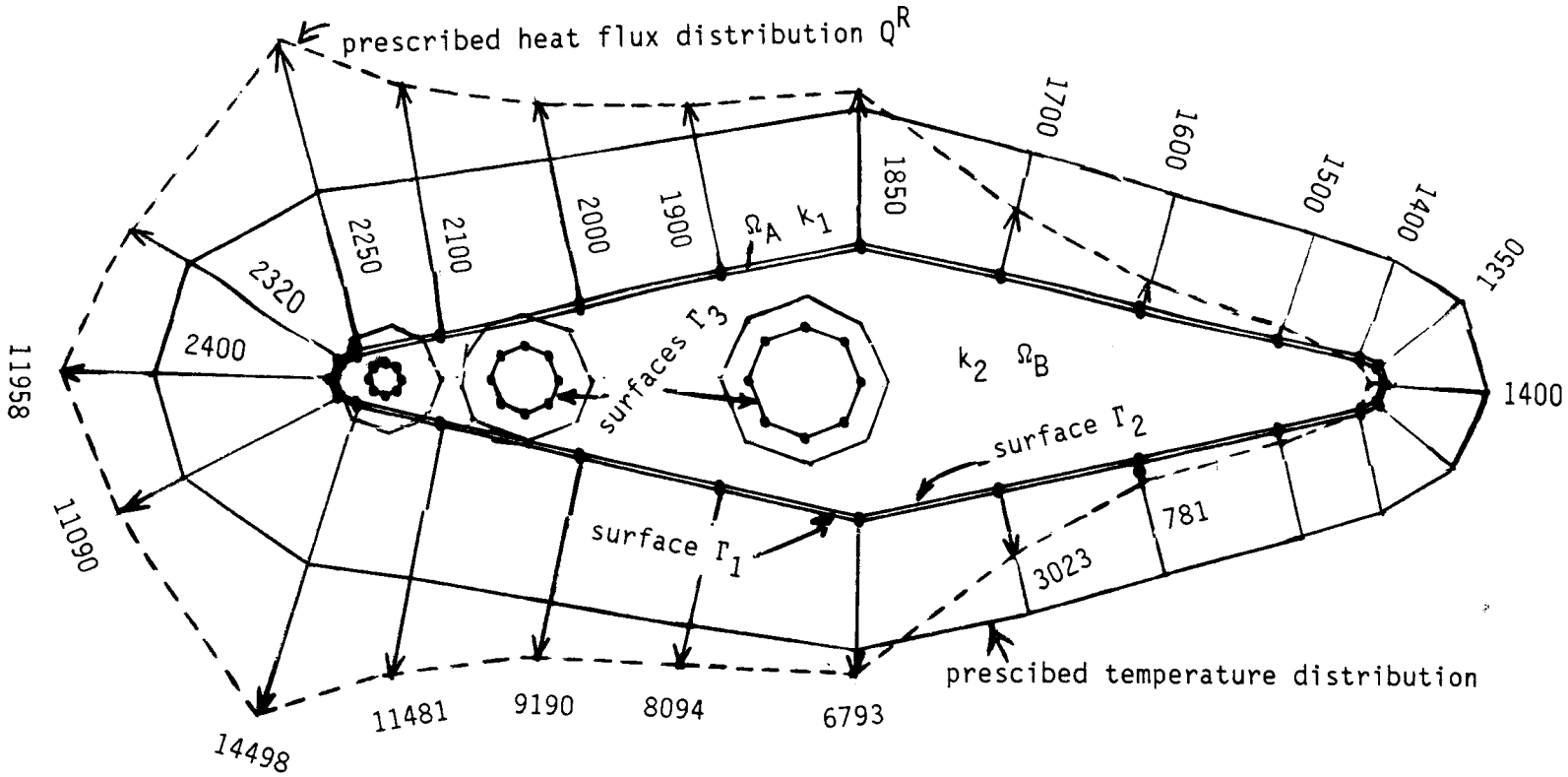

Fig. 1 Discretized Ceramically Coated Scram Jet Combustor strut
With prescribed Temperatures and Outer Surface Heat Flux
chord length of the strut : 19.
maximum thickness of the strut : 5.

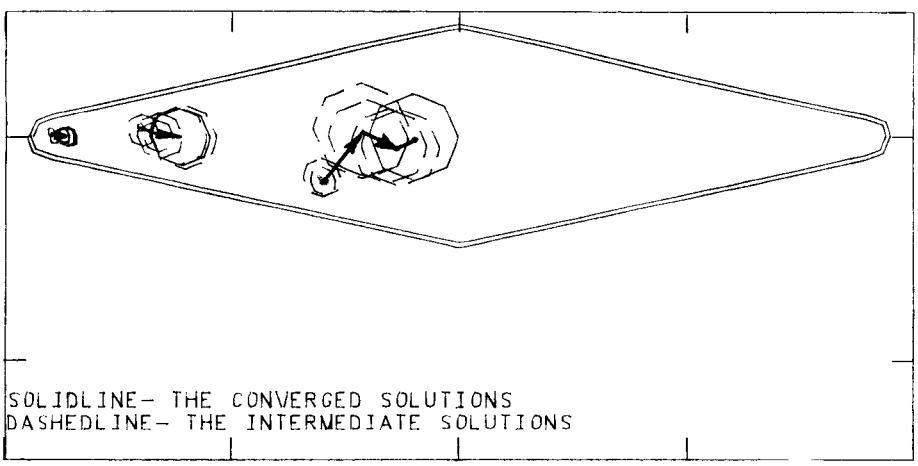

Fig. 2 Iteration sequence of case 1 (norm error = 0.554 %)

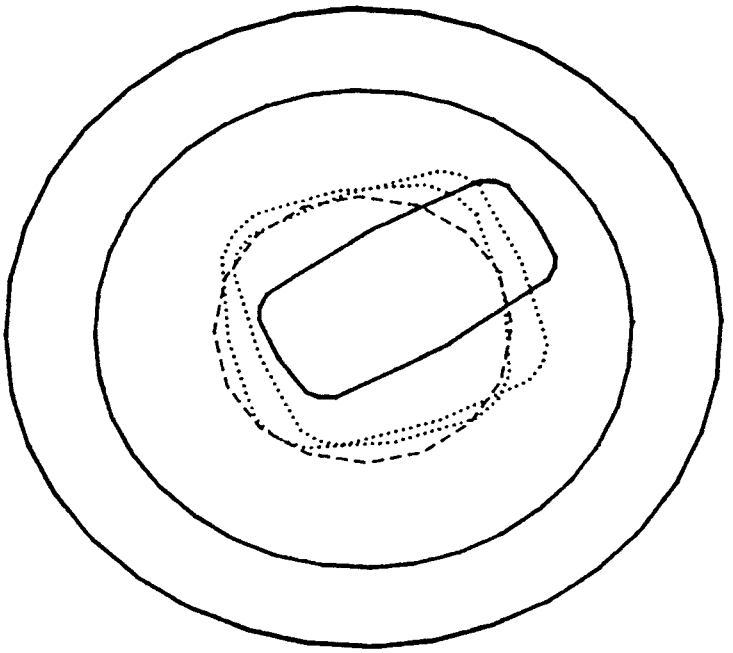

Fig. 2.1 Initial configuration (an off-center inclined almost rectangular hole) and optimized configuration (one large centrally located hole) for one-hole coated disk with intermediate hole shapes.

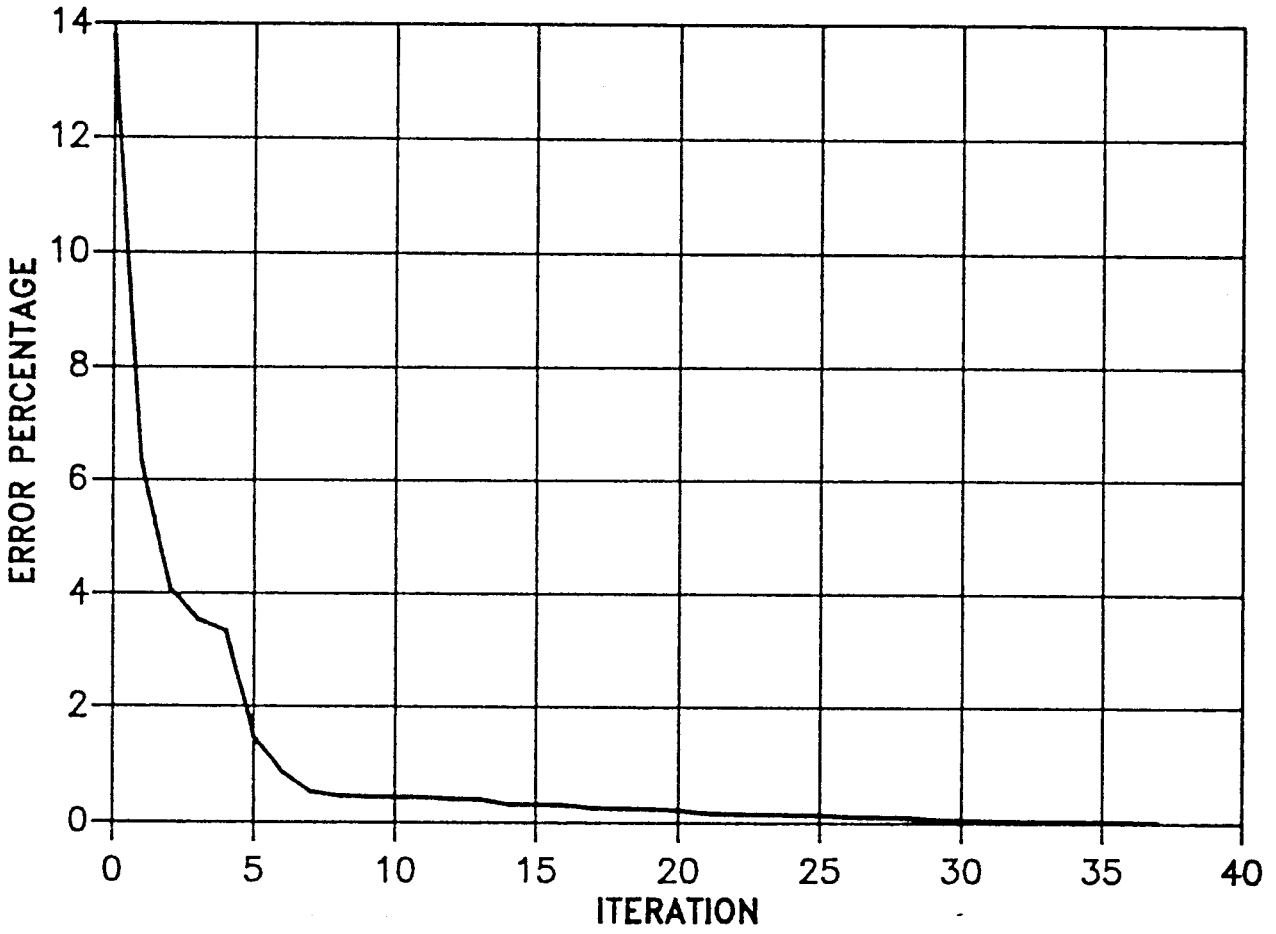

Fig. 2.2 Convergence history of the coated disk with one-hole configuration.

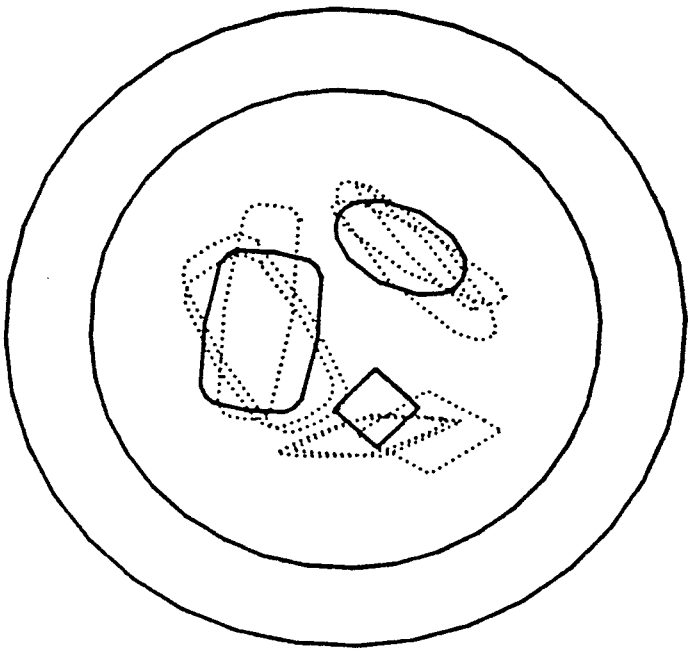

Fig. 2.3 Initial configuration consisting of three different holes (solid line) and their inermediate shapes during the first 64 optimization cycles for a coated disk.

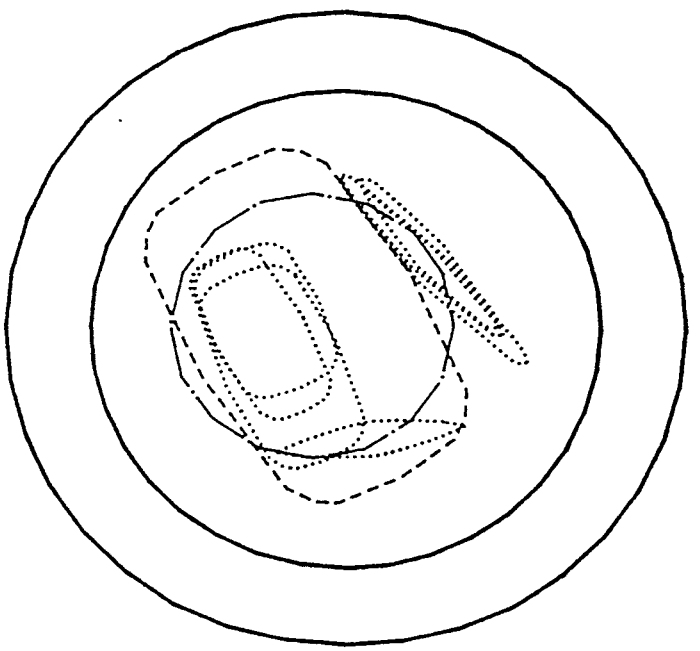

Fig. 2.4 Inermediate shapes of the three different holes during the optimization cycles 65-121 for a coated disk.

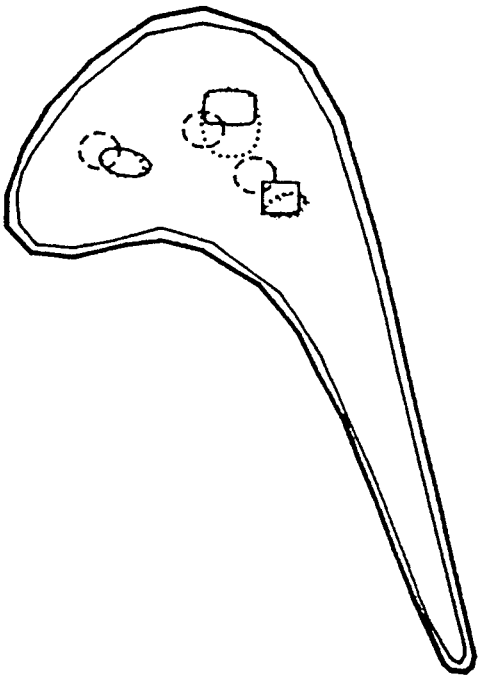

Fig. 2.5 Initial configuration (three circular holes) and optimized configuration (ellipse, rectangle, and a square) for a coated turbine blade with intermediate hole shapes (dotted).

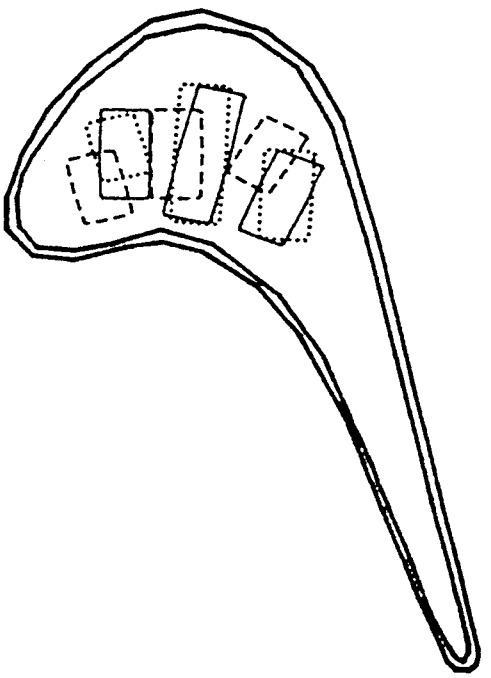

Fig. 2.6 Initial configuration (three unequal almost rectangular holes) and optimized configuration (three diffeently sized, positioned almost rectangular partially constrained holes) for the coated turbine blade airfoil with intermediate hole shapes.

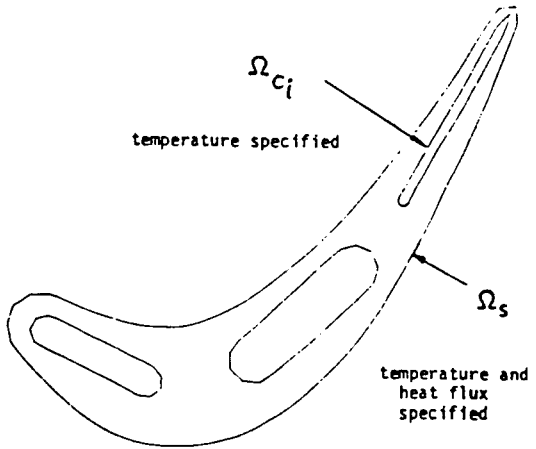

Fig. 1. Geometry and boundary conditions /9/.

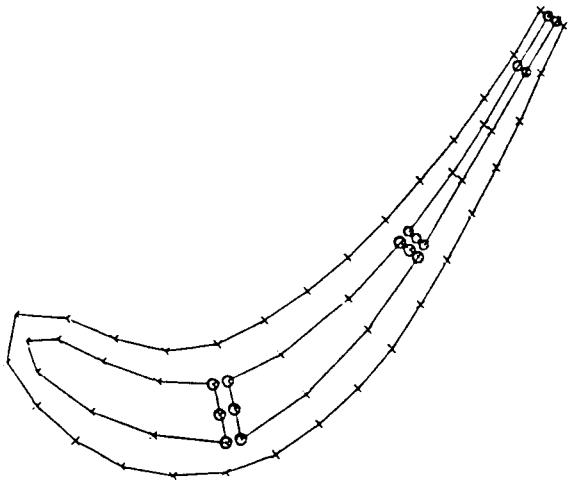

Fig. 2. Inner and outer contours discretized with panels (O denotes fixed end points).

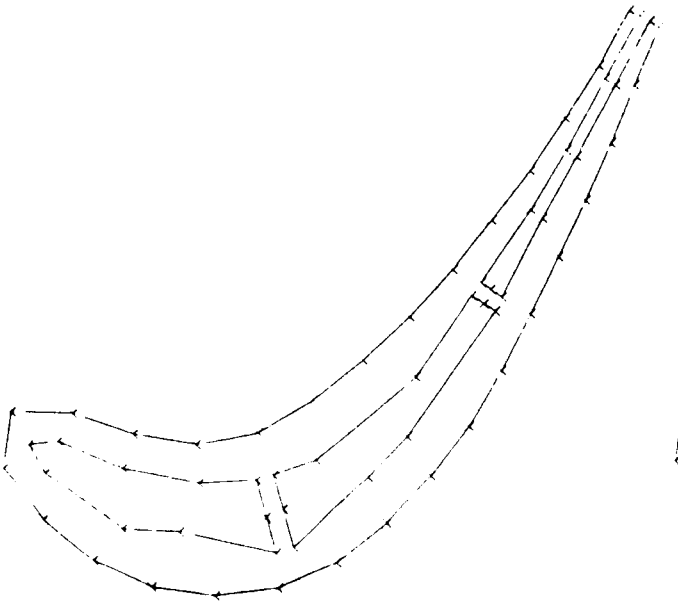

Fig. 4. Turbine design for case 1.

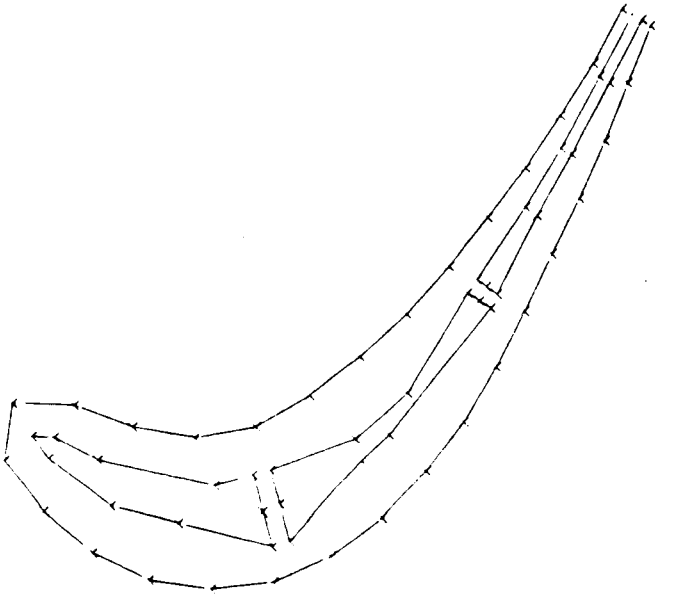

Fig. 5. Turbine design for case 2.

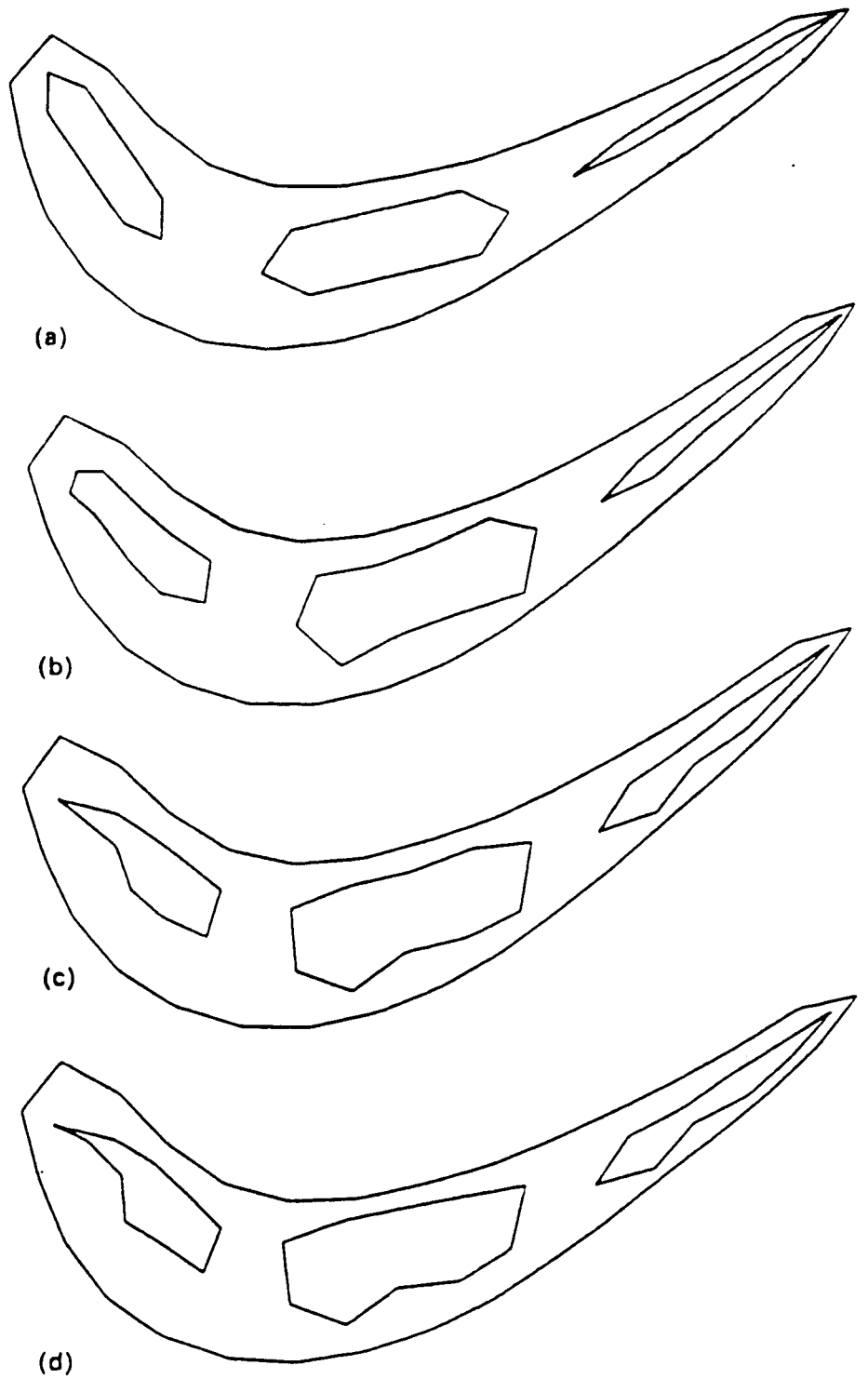

. Iteration sequence for turbine design case 1: (a) initial configuration; (b) solution after 6 iterations; (c) solution after 14 iterations; (d) solution after 18 iterations